International Journal of Pharmaceutics 396 (2010) 91–98

Contents lists available at ScienceDirect

International Journal of Pharmaceutics

journal homepage: www.elsevier.com/locate/ijpharm

Enhanced dissolution of megestrol acetate microcrystals prepared by antisolvent precipitation process using hydrophilic additives

Eunbi Cho, Wonkyung Cho, Kwang-Ho Cha, Junsung Park, Min-Soo Kim, Jeong-Soo Kim, Hee Jun Park, Sung-Joo Hwang*

Center for Nanotechnology-based New Drug Dosage Form, College of Pharmacy, Chungnam National University, 220 Gung-dong, Yuseong-gu, Daejeon 305-764, Republic of Korea

ARTICLE INFO

Article history:
Received 30 March 2010
Received in revised form 27 May 2010
Accepted 9 June 2010
Available online 15 June 2010

Keywords:
Megetsrol acetate
Microcrystals
Antisolvent precipitation
Hydrophilic additives
Dissolution properties

ABSTRACT

Microcrystals of megestrol acetate (MA), a poorly water-soluble drug, were successfully prepared using an antisolvent precipitation technique for improving the dissolution rate. The effective hydrophilic polymers and surfactants used were screened for their abilities to produce smaller particle sizes. Raw micronized MA and processed MA microcrystals were ranked by the Student–Newman–Keuls test in order of increasing particle size and SPAN values as follows: processed MA microcrystals in the presence of polymer and surfactant (mean diameter 1048 nm) < processed MA microcrystals in the presence of polymer (1654 nm) < processed MA microcrystals in the absence of polymer and surfactant (3491 nm) < raw micronized MA (4352 nm). The order of BET surface area was reversely ranked. Processed MA microcrystals in the presence of polymer and surfactant slightly decreased crystallinity and altered crystal habit and preferred orientation without change in polymorph. In addition, the dissolution properties of the processed MA microcrystals in the presence of polymer and surfactant were significantly enhanced as compared to that of the raw micronized MA. This effect is mainly due to a reduction in particle size resulting in an increased surface area. Therefore, it was concluded that the antisolvent precipitation technique in mild conditions could be a simple and useful technique to prepare poorly water-soluble drug particles with reduction in particle size, a narrow particle size distribution and enhanced dissolution properties.

1. Introduction

Megestrol acetate (MA), 17α-acetyloxy-6-metylpregna-4,6-diene-3,20-dione, is a synthetic progestin and has the molecular structure shown in Fig. 1. It has progestational effects similar to those of progesterone and is used for abortion, endometriosis, menstrual disorders, breast cancer treatment, contraception and hormone replacement therapy in post-menopausal women. In addition, it is frequently prescribed as an appetite enhancer for patients in a wasting state, such those with HIV wasting, cancer wasting or anorexia (Mateen and Jatoi, 2006).

According to the biopharmaceutical classification system (BCS) (Löbenberg and Amidon, 2000), MA is a BCS class II drug, which has poor water solubility and high permeability (Rasenack et al., 2003). Enhancing the dissolution rate of poorly water-soluble drugs in order to increase the rate and extent of drug absorption is essential for optimizing the bioavailability (Kocbek et al., 2006; Huang et al., 2008). Several techniques are commonly used to improve the dissolution rate and bioavailability of poorly water-soluble drugs including size reduction (Perrut et al., 2005), the use of surfactants (Raghavan et al., 2001; Goddeeris et al., 2007), the transformation of a crystalline drug into an amorphous state (Goddeeris et al., 2008) and the formation of solid dispersions (Leuner and Dressman, 2000). According to the Noyes–Whitney equation, the dissolution rate of drugs can be increased by reducing the their particle size at the micro- or nano-scale to increase the surface area of drug particles (Mosharraf and Nyström, 1995). Previous studies with many poorly water-soluble drugs have demonstrated that particle size reduction can lead to an increase in dissolution rate and a higher oral bioavailability (Hargrove et al., 1989; Watari et al., 1983).

The existing technologies for reducing particle size can be divided into so-called "top down" and "bottom-up" technologies. The top down technologies involve the mechanical comminution of previously formed larger particles such as jet milling, pearl mill and spiral jet milling (Midoux et al., 1999), as well as some new techniques including media milling technology (Merisko-Liversidge et al., 2003) and high pressure homogenization (Keck and Muller, 2006). However, none of these technologies are ideal for the formation of microcrystal particles because they are usually inefficient due to high energy input or pharmaceutical contamination and denaturation during the milling process (Vivek et al., 2006). Bottom-up technologies include precipitation-based pro-

* Corresponding author. Tel.: +82 42 821 5922; fax: +82 42 823 3078.
E-mail address: sjhwang@cnu.ac.kr (S.-J. Hwang).

0378-5173/$ – see front matter © 2010 Elsevier B.V. All rights reserved.
doi:10.1016/j.ijpharm.2010.06.016

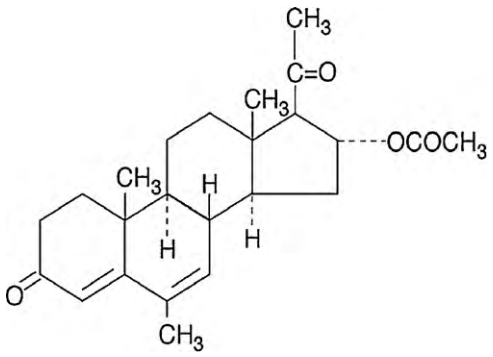

Fig. 1. Structure of megestrol acetate.

cesses like spray drying and supercritical antisolvent process (Kim et al., 2008b), spray freeze drying into liquid (Kondo et al., 2009), evaporative precipitation into aqueous solution (Chen et al., 2002; Sarkari et al., 2002) and the liquid solvent change process (Rasenack and Muller, 2004).

For MA, submicron particles have been prepared using wet-milling technology (Hovey et al., 2005). Especially, nanocrystal oral suspension using a wet-milling technology is commercially marketed by Megace® ES from Par Pharmaceutical (Hovey et al., 2005). However, these techniques are inefficient due to previously mentioned disadvantages during the milling process. And ultrafine MA particles have been produced by supercritical fluid extraction of emulsions (Shekunov et al., 2006; Dukhin et al., 2007). This method, however, has limitations, e.g. low yield, high equipment cost (Perrut and Clavier, 2003; Wang et al., 2007). On the other hand, the antisolvent precipitation method, one of the bottom-up technologies, is an effectively applicable way to prepare micro- or nano-sized drug particles because the technique is performed under cost-effective and the mild process conditions that do not require high temperature and high pressure. Furthermore, it is well suited to scaling up for production of large amounts of drug compared to spray drying and supercritical fluid technology, spray-freezing into liquid (Ruch and Matijevic, 2000; Cushing et al., 2004).

In this study, we prepared MA microcrystals using an antisolvent precipitation technique in the presence of polymer and surfactant for the enhancement of the dissolution rate. Furthermore, the effective hydrophilic polymers and surfactant used were screened for their abilities to produce smaller particle sizes, resulting in enhanced dissolution rates. Physical properties of raw micronized MA and MA microcrystals prepared by antisolvent precipitation technique were characterized in the solid state using several techniques such as dynamic light scattering (DLS), scanning electronic microscopy (SEM), Fourier transformation-infrared spectroscopy (FT-IR), differential scanning calorimetry analysis (DSC), powder X-ray diffraction analysis (PXRD), BET surface area analysis, kinetic solubility and dissolution test.

2. Materials and methods

2.1. Materials

Raw MA was purchased as a commercial micronized grade (mean particle size 4352 nm) for oral suspension from Taizhou Baida Pharmaceutical Co., Ltd., China. Hydroxypropyl methyl cellulose (HPMC 2910) was provided by Samsung Fine Chemicals Co., Ltd., Korea. Vinylpyrrolidon-vinyl acetate-copolymerisat K28 (Kollidon VA 64), Ethylene oxide-propylene oxide block copolymer (Poloxamer 407) and Polyvinylpyrrolidone K90 (PVP K90) were purchased from BASF Co., Ltd., Germany. Polyvinylalcohol (PVA, mol. wt. 31,000–50,000) was bought from Sigma Chemical Co., USA. Polyoxyethylene (20) sorbitan monolaurate (Tween 20), polyoxyethylene (60) sorbitan monolaurate (Tween 60), polyoxyethylene (80) sorbitan monolaurate (Tween 80) and acetone were purchased from Samchun Chemical Co., Korea.

2.2. Preparation of MA microcrystal particles

MA microcrystals particles were prepared using an antisolvent precipitation technique. A certain concentration of MA was completely dissolved in solvent (1 ml acetone). The prepared drug solution was injected by syringe into 20 ml water containing each specific concentration of polymer and surfactant with stirring at 1500 rpm. Precipitation of drug particles occurred immediately upon mixing and formed a suspension with a milky appearance. The suspension was centrifuged at 5000 rpm ($4582.3 \times g$, "g" represents the gravitational acceleration, $9.81\ m\ s^{-2}$) for 5 min with a centrifuge (MF550, Hanil Science Industrial, Korea) and washed twice with 10 ml deionized water. The obtained particles were oven-dried at 50 °C overnight.

2.3. Size measurement

Particle size and distribution of samples were determined by dynamic light scattering (DLS) using an electrophoretic light scattering spectrophotometer (ELS-8000, Otsuka Electronics, Japan). The MA samples were dispersed in deionized water by sonicating for 1 min. Each measurement was performed in triplicate. The DLS data was analyzed using the cumulant method, we obtained information about particle size. The particle size distribution was also estimated from the correlation function profile using histogram analysis.

2.4. Scanning electron microscopy (SEM)

The morphology of the particles was observed using a scanning electron microscope (SEM; JSM-7000F, Jeol Ltd., Japan). MA samples were coated with gold and palladium using a vacuum evaporator and examined using an SEM at a 15 kV accelerating voltage.

2.5. Fourier transformation-infrared spectroscopy (FT-IR)

FT-IR spectroscopy was conducted on a FT-IR spectrometer (Thermo Fisher, Nicolet 380 T-IR, USA) using the attenuated total reflectance (ATR) method. The scanning range was 650–4000 cm^{-1} and the resolution was 4 cm^{-1}. A total of 32 reference scans were performed.

2.6. Thermal analysis

DSC measurements were carried out in a DSC S-650 (Scinco Co. Ltd., Korea). MA samples of 2–3 mg were accurately weighed and sealed in aluminum. The measurements were performed under nitrogen purge over 20–300 °C at a heating rate of 20 °C/min. The onset, melting points and enthalpies of fusion were automatically calculated by the instrument. An empty pan was used for reference and calibration prior to each experiment. A nitrogen flow rate of 20 °C/min was used for each DSC run. Thermal gravimetric analysis (TGA) was carried out using a 2940TMA (TA Instruments, USA). MA samples weighing 2–3 mg were heated at a rate of 10 °C/min under a nitrogen purge.

2.7. Powder X-ray diffraction analysis

The PXRD patterns of MA samples were recorded in a Rigaku powder X-ray diffraction system (Model D/MAX-2200 Ultima/PC,

Japan) with Ni-filtered Cu-Kα radiation. The samples were run over the most informative range from 5° to 70° of 2θ. The step scan mode was performed with a step size of 0.02° at a rate of 2°/min.

2.8. Specific surface area

The specific surface area was measured using the N_2 adsorption method. In this method, calculation was performed by the Surface Area Analyzer (ASAP 2010-M, Micromeritics Instrument Co., USA) based on the BET equation. Before measuring, the sample powders were degassed for at least 4 h.

2.9. Drug content

MA microcrystal particles obtained by antisolvent precipitation of 5 mg were dissolved in a suitable quantity of acetonitrile. The drug content was determined by HPLC system (Waters, USA) consisting of a pump (Model 600), an auto-sampler (Model 717 plus) and UV detector (Model 486 Tunable Absorbance Detector), which was equipped with the X-Terra™RP C^{18}Column (5 μm 4.6 mm × 250 mm). The mobile phase, composed of 65% acetonitrile and 35% deionized water (v/v), was delivered at 1.0 ml/min. The drug was detected at 280 nm and the retention time of the drug was 6.6–6.8 min.

2.10. Kinetic solubility test

For the kinetic solubility test, an excess amount (5 mg) of raw micronized MA or processed MA microcrystals was placed in 10 ml deionized water in a test tube. Test tubes were placed in a shaking water bath and were shaken (70 rpm) at 37 ± 0.1 °C. Appropriate aliquots were withdrawn at certain time intervals (5 min, 1, 2, 4, 6, 8, 12 and 24 h) using a 1 ml syringe and were filtered using 0.2 μm PTFE filters. Filtered samples were diluted with acetonitrile and the concentration of MA was determined by an HPLC system.

2.11. Dissolution test

The dissolution studies were performed following the USP, Apparatus 2 (paddle) method (UDT 804; LOGAN Instruments Co., USA). The paddle speed and bath temperature were set to 50 rpm and 37.5 ± 0.5 °C, respectively. Each test was carried out in 900 ml of 0.25% SLS dissolution medium for the sink condition. Accurately weighed samples containing the equivalent of 50 mg raw micronized MA or the processed MA microcrystals were placed in the dissolution medium. Then, 2 ml aliquot samples were withdrawn at the specified time intervals and were filtered using 0.45 μm PTFE syringe filters. At each sampling time, an equal volume of the test medium was transferred. One-half milliliter of each filtered sample was diluted with mobile phase and assayed for drug concentration by HPLC.

2.12. Statistical analysis

The statistical significances of differences among formulations were estimated using one-way analysis of variance (ANOVA) followed by Tukey's test and the Student–Newman–Keuls test in terms of particle size, BET surface area, drug dissolution efficiency and percent of drug dissolved at a given time using SPSS 12.0 for Windows (SPSS, Chicago, IL, USA).

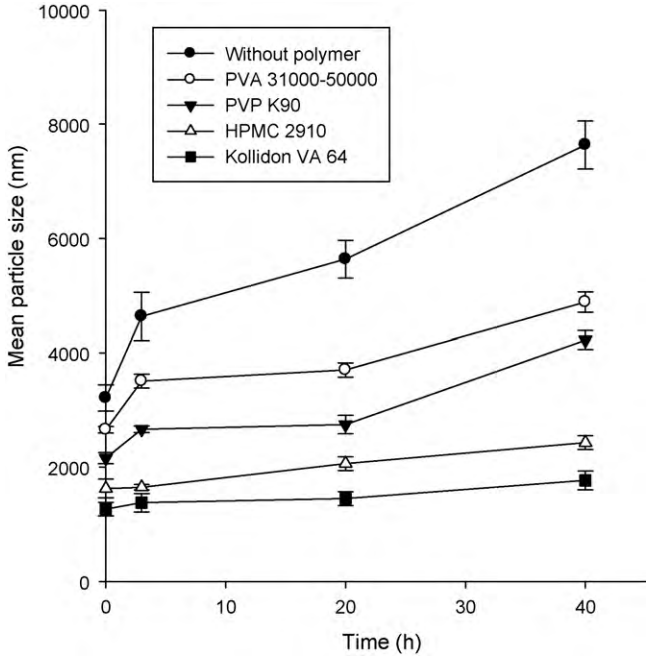

Fig. 2. Changes in particle size of MA particles processed by antisolvent precipitation technique.

3. Results and discussion

3.1. Screening study of polymer and surfactant

3.1.1. Effect of polymer

The polymer screening was performed using assorted polymers including PVP K90, PVA 31,000–50,000, Kollidon VA 64 and HPMC 2910 in deionized water (0.2%, w/v) at a constant drug concentration (90 mg/ml). The change in particle size of the precipitated drug particles in suspension was measured over time. Fig. 2 shows that the use of a polymer had an effect on inhibition of crystal growth compared to prepared particles without polymer. Although the energy of the van der Waals attraction that is proportional to particle radius occurs (Russel et al., 1989), the suspension with polymer had the higher zeta potential value (−20.68 ± 1.51 mV) than that of suspension without the hydrophilic additives (−3.7 ± 3.37 mV). This elucidates the effect of polymer on the MA suspension stability. The small particles such as microcrystals, which normally would aggregate in order to lower the surface energy, are stabilized sterically against crystal growth by a layer of protective polymer (Rasenack et al., 2003; Zimmermann et al., 2009). Furthermore, the use of polymer as a crystal growth inhibitor for steroid drugs having similar structures to MA has been reported in previous studies (Dong et al., 2009; Ali et al., 2009). Among the polymers used, Kollidon VA 64 was the most effective for inhibition of crystal growth. This result may be due to the high affinity of the MA particle for this polymer. Therefore, it provided an effective steric barrier against crystal growth. From the polymer screening, Kollidon VA 64 was selected as a stabilizer for the rest of the experiments.

3.1.2. Effect of surfactant

MA microcrystals were prepared by antisolvent precipitation using various surfactants such as Poloxamer 407, Tween 20, Tween 60 and Tween 80 under a constant concentration of the surfactant (0.1%, w/v), Kollidon VA 64 (0.2%, w/v) and drug (100 mg/ml). Table 1 shows that the use of surfactant was effective for decreasing the particle size of MA microcrystals. This effect can be explained by the fact that the addition of surfactants may contribute to a

Table 1
Influence of various surfactant on MA mean particle size.

	Without surfactant	Tween 20	Tween 60	Tween 80	Poloxamer 407
Mean particle size ± SD (nm)	2909 ± 125.6	2348 ± 100.5	2036 ± 80.42	2069 ± 118.0	1749 ± 35.70

reduction in mean particle size due to the surface-active properties of the surfactants (Lim and Kim, 2002; Park et al., 1999; Won et al., 2005). The analysis of variance showed that there were significant differences in particle size among the formulations that used or omitted surfactant ($P < 0.001$). The most effective surfactant among those screened was Poloxamer 407. Particularly, a combination of several stabilizers is often used in order to achieve optimal effect (Chen et al., 2010). Block co-polymeric surfactant such as Poloxamer 407, consists of ethylene glycol and propylene glycol, are very efficient non-ionic stabilizers owing to multiple attachments of hydrophobic domains at the drug particle surface (Kipp, 2004). Because Poloxamer 407 has hydrophobic moieties that adsorb onto hydrophobic drug particle surface and two hydrophilic blocks, the adsorption of Poloxamer 407 with Kollidon VA 64 may be expected to provide greater steric repulsion and inhibition of aggregation corresponding to the higher zeta potential value (−26.66 ± 2.30 mV) compared to those of suspension with polymer and without hydrophilic additives (Chen et al., 2009).

3.1.3. Effect of drug concentration

As shown in Fig. 3, an increase in drug concentration from 30 to 120 mg/ml resulted in a decrease in particle size from 4190 to 1048 nm. A higher drug concentration could create a higher supersaturation level and a faster nucleation rate, resulting in smaller particle sizes (Dong et al., 2009; Matteucci et al., 2006). In contrast, drug concentrations above 120 mg/ml yielded increased particle sizes and span values. Too great of an increase in drug concentration in solution can lead to an increase in viscosity, which can prevent diffusion between solution and antisolvent and has been shown to result in nonuniform supersaturation and agglomeration (Zhang et al., 2006).

3.1.4. Effect of Kollidon VA 64 concentration

The average particle sizes of the MA samples were measured at different concentrations of polymer (Kollidon VA 64). Fig. 4 shows that a polymer concentration of 0.2% (w/v) yielded the smallest particle size. However, the particle size increased as the concentration of polymer increased to greater than 0.2% (w/v). This result might be due to inhibiting an appropriate diffusion of the solvent toward the antisolvent caused by the high viscosity of the solution containing polymer (Bilati et al., 2005). Increasing particle sizes achieved with higher polymer concentrations have also been reported by other investigators (Labouret et al., 1995; Stainmesse et al., 1995; Thioune et al., 1997).

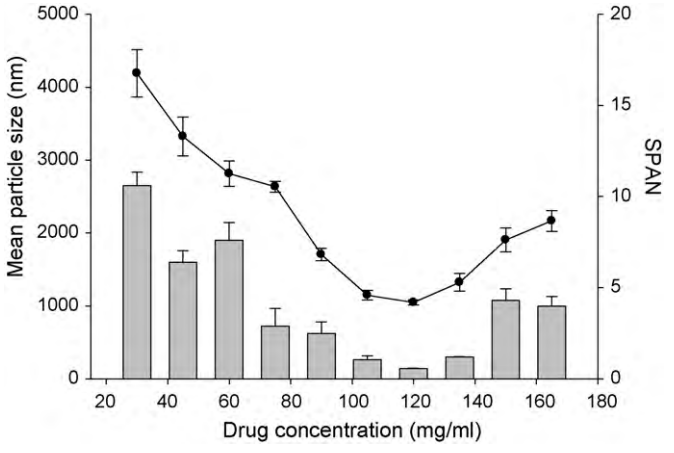

Fig. 3. Effect of drug concentration on the mean particle size (●) and SPAN value of processed MA microcrystals (vertical bar means SPAN value).

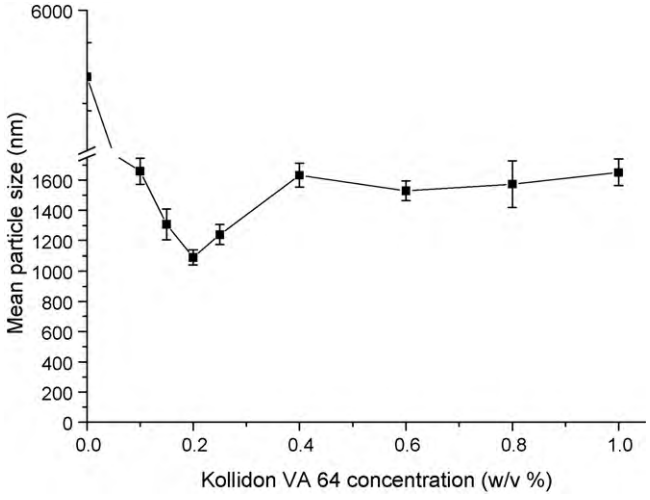

Fig. 4. Effect of Kollidon VA 64 on the mean particle size of processed MA microcrystals.

3.2. Characterization of the MA microcrystal particles

As shown in Table 2, raw micronized MA and 3 processed MA microcrystals (M1–M3) were prepared and characterized on the basis of our previous experiences with the antisolvent precipitation technique.

3.2.1. Morphology and particle size distribution

SEM images of raw micronized MA and processed MA microcrystal particles are shown in Fig. 5. The M3 microcrystals appear uniform and plate-like, while the raw micronized MA appears needle-like with irregularly shaped crystals several microns in size. The M1 microcrystals had an irregular appearance with large aggregates and the M2 microcrystals showed irregular particles including aggregate particles with both needle-like and plate-like appearances. The particle size and specific surface area data of raw micronized MA, M1, M2 and M3 are summarized in Table 3. Analysis of variance showed that there were significant differences in the particle size distributions among MA samples from each precipitation condition (Fig. 6). The BET surface areas among the MA samples also showed significant differences ($P < 0.05$), which were ranked by the Student–Newman–Keuls test in order of increasing particle size and SPAN values as follows: M3 < M2 < M1 < raw micronized MA. The order of BET surface area was reversely ranked (raw micronized

Table 2
Precipitation conditions of major processed MA microcrystals.

Sample	MA (mg/ml)	Aqueous solution composition	
		Kollidon VA 64 (w/v%)	Poloxamer 407 (w/v%)
M1	120	–	–
M2	120	0.2	–
M3	120	0.2	0.1

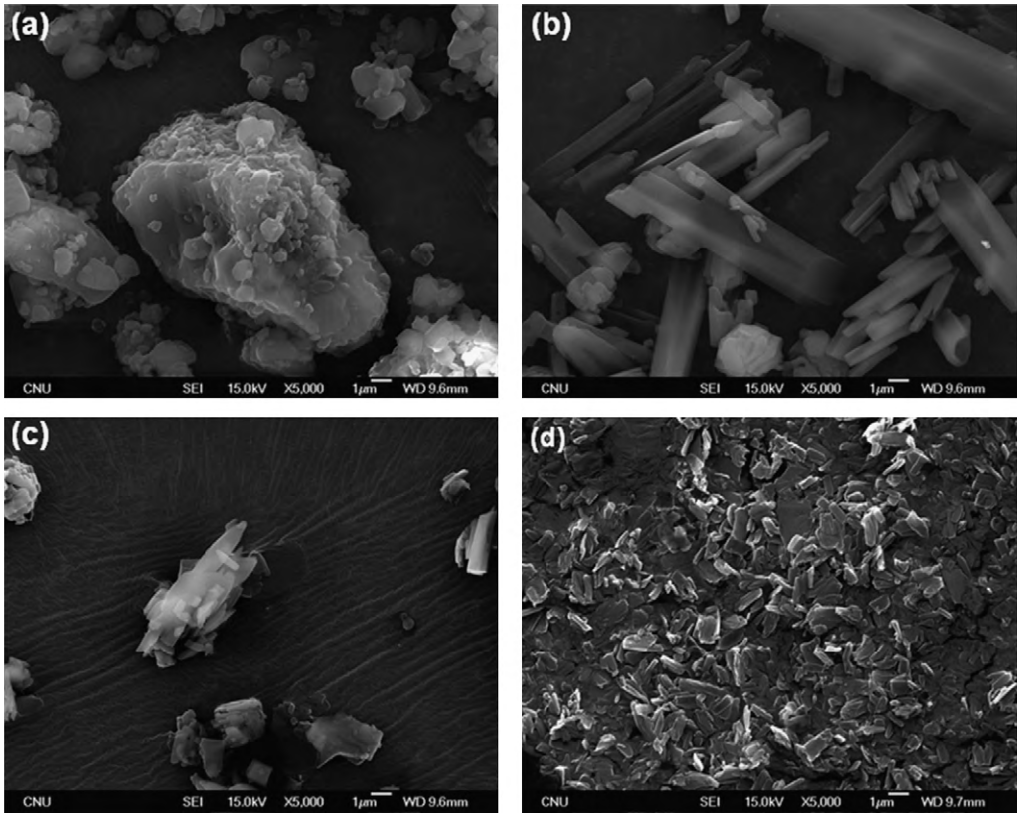

Fig. 5. SEM images of (a) raw micronized MA, (b) M1, (c) M2 and (d) M3.

Table 3
Mean particle sizes and BET surface area of raw micronized MA and processed MA microcrystals.

Sample	Mean particle size[a] (nm)	SPAN[b]	BET surface area (m^2/g)
Raw micronized MA	4352 ± 313.8	10.77	2.224 ± 0.021
M1	3491 ± 148.5	5.135	2.932 ± 0.006
M2	1654 ± 49.70	3.362	3.646 ± 0.023
M3	1048 ± 19.80	0.861	4.802 ± 0.080

[a] Mean particles size calculated by cumulative method using dynamic light scattering measurement ($n = 3$).
[b] SPAN = $D_{90} - D_{10}/D_{50}$.

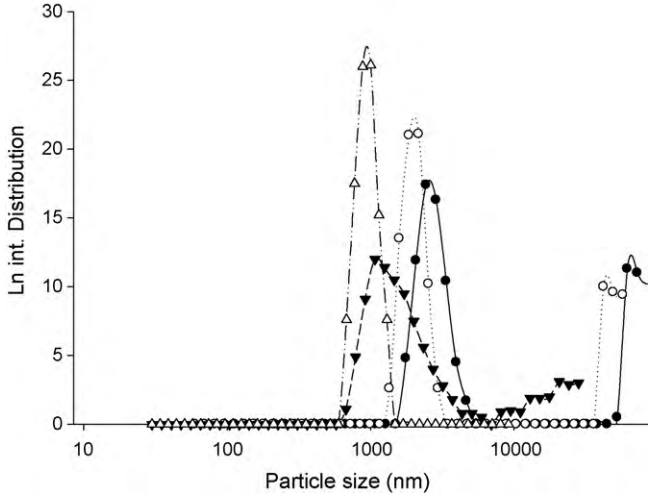

Fig. 6. Particle size distribution of raw micronized MA (●), M1 (○), M2 (▼) and M3 (△).

MA < M1 < M2 < M3). These results showed that addition of polymer and/or surfactant in aqueous phase had an effect on particle size distribution and that processed MA microcrystals in the presence of polymer and surfactant (M3) provided the best results.

3.2.2. DSC analysis

The changes in polymorphism and crystallinity of MA before and after the antisolvent precipitation process were assessed by comparing the DSC thermograms (Fig. 7) and PXRD patterns (Fig. 8) of all MA samples. DSC data for 4 samples are shown in Table 4. The DSC thermograms of all samples showed a peak at 216–217 °C, which corresponded to the melting point of MA. As shown in Fig. 7, the

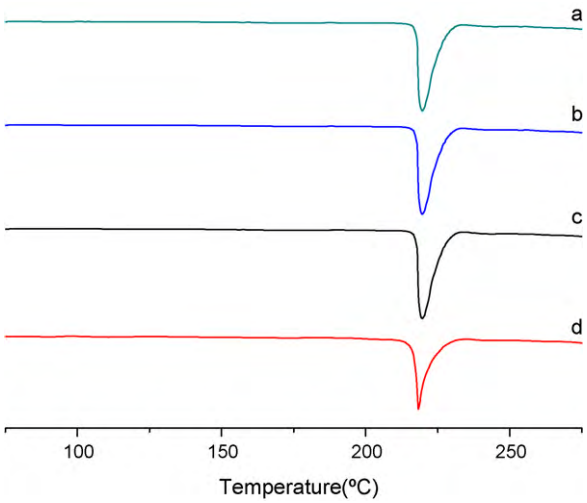

Fig. 7. DSC thermograms of (a) raw micronized MA, (b) M1, (c) M2 and (d) M3.

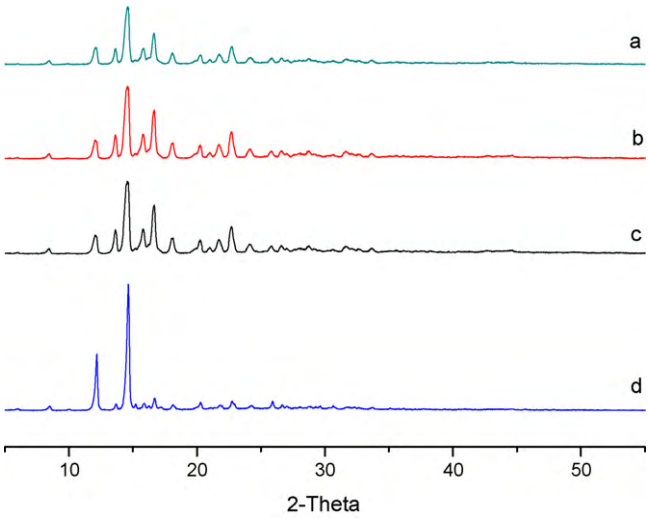

Fig. 8. PXRD patterns of (a) raw micronized MA, (b) M1, (c) M2 and (d) M3.

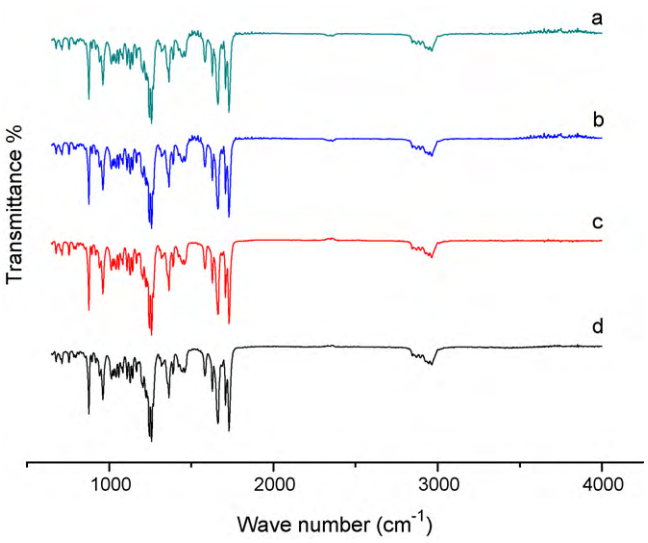

Fig. 9. FT-IR spectra of (a) raw micronized MA, (b) M1, (c) M2 and (d) M3.

enthalpy of M3 was decreased compared to those of raw micronized MA, M1 and M2, which were almost identical. The reduced enthalpy of the M3 microcrystals indicates a decreased crystallinity for crystal particles obtained in the presence of polymer and surfactant (Dong et al., 2009).

3.2.3. PXRD analysis

Fig. 8 shows that all MA samples had the same polymorph with similar peak positions in the PXRD patterns. However, there were some differences among MA samples in the relative integrated intensities of each peak. These differences can be explained by preferred orientation, in which the distribution of crystal orientation is nonrandom and crystals may tend to grow greater or lesser degree to specific orientation (Yeo et al., 2003; Park et al., 2007). The orientation of some particular molecular arrangements corresponding to peaks at 12.18° and 14.56° was more preferred in M3 than it was in the other samples. This result might be attributable to a difference not of polymorph, but of crystal habit. The difference could be because the abundance of the planes exposed to the X-ray source would have been changed, thus producing the change in the relative intensities of the peak (Marshall and York, 1989; Nokhodchi et al., 2003).

3.2.4. FT-IR analysis

Fig. 9 shows that all MA samples have the same FT-IR spectrum. These findings confirmed the results of the PXRD analysis that all MA samples were of the same polymorph.

3.2.5. Drug content study

The drug contents of the MA microcrystals were above 99% for all MA samples. These results show that almost all of the Kollidon VA 64 and Poloxamer 407 were removed by washing. Furthermore, there was no mass loss of residual solvent during the TGA experiments (data not shown). Therefore, we conclude that residual solvent, polymer and surfactant were not present in the particles prepared in this study, consistent with the results of the DSC, PXRD and FT-IR analyses.

Table 4
DSC data of raw micronized MA and processed MA microcrystals ($n = 3$).

Type of crystal samples	Fusion temperature (°C)	Enthalpy of fusion (J/g)
Raw micronized MA	217.09 ± 1.02	84.63 ± 1.93
M1	216.98 ± 1.08	84.77 ± 1.77
M2	216.98 ± 0.08	85.01 ± 1.69
M3	217.02 ± 0.03	78.11 ± 1.02

3.2.6. Kinetic solubility and dissolution results

The kinetic solubility test for each MA sample was performed over 24 h. Fig. 10 shows that the maximum solubility of M3 was much higher than those of the other MA samples. The results seemed to be due to a decrease in crystallinity. That is explained by that a solid having a higher lattice free energy will tend to increase the solubility and hence the driving force for dissolution (Blagden et al., 2007; Brittain, 1999). Furthermore, the maximum concentration of the MA samples in solution decreased over time, caused by a solvent-mediated conversion to the crystal with the higher crystal perfection (Kim et al., 2008a).

The results of the dissolution experiments are illustrated in Fig. 11 and summarized in Table 5 in terms of the percent dissolved (PD) after 5, 10 and 30 min and in terms of dissolution efficiency (DE) at 60 min. Statistical analysis of all dissolution parameters showed that for all of the examined MA samples, the rank order obtained by the Student–Newman–Keuls test in terms of both PD and DE was always M3 > M2 > M1 > raw micronized MA ($P < 0.001$). This result corresponds to the order calculated for BET surface area

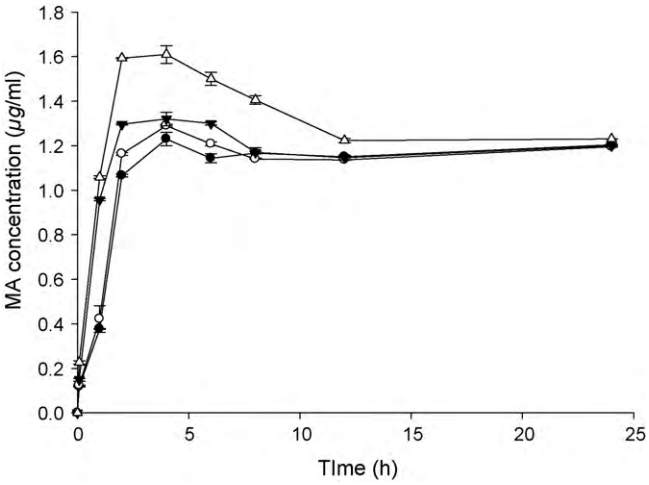

Fig. 10. Kinetic solubility profiles of raw micronized MA (●), M1 (○), M2 (▼) and M3 (△) ($n = 3$, mean ± SD).

Table 5
Percent dissolved (PD) at 5, 10, 30 min and dissolution efficiency (DE)[a] at 60 min of raw micronized MA, M1, M2 and M3 ($n = 3$, mean ± SD).

Sample	PD 5	PD 10	PD 30	DE[a] 60
Raw micronized MA	47.7 ± 3.10	57.3 ± 2.24	69.1 ± 2.36	65.9 ± 1.35
M1	51.1 ± 1.37	62.6 ± 1.38	78.9 ± 1.40	73.7 ± 0.82
M2	68.3 ± 1.02	78.4 ± 1.20	90.2 ± 0.05	84.5 ± 0.96
M3	87.7 ± 0.69	97.9 ± 1.07	99.9 ± 2.43	95.9 ± 0.42

[a] Calculated from the area under the dissolution curve at 60 min and expressed as % of the area of the rectangle described by 100% dissolution in the same time.

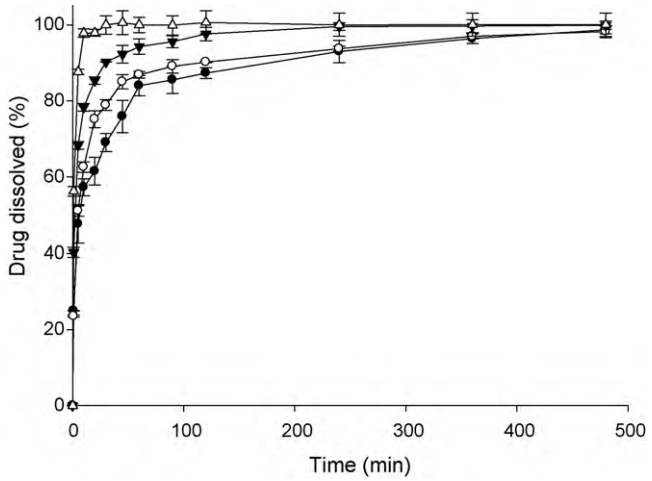

Fig. 11. Dissolution profiles of raw micronized MA (●), M1 (○), M2 (▼) and M3 (△) ($n = 3$, mean ± SD).

and the reversed order for particle size. The dissolution results were likely due to a reduction in particle size resulting in an enlarged surface area for the drug (from 2.2241 to 4.8020 m^2/g), which consequently increased the dissolution velocity as described by the Noyes–Whitney equation (Noyes and Whitney, 1897). In particular, M3 samples showed significantly improved drug dissolution parameters (Table 5) as compared to those of the other MA samples ($P < 0.001$) because of increasing the surface area caused by a reduction in particle size and decreased crystallinity. Overall, the results of these experiments showed conclusively that a reduction in particle size using an antisolvent precipitation technique can improve the dissolution properties of MA.

4. Conclusion

In this study, microcrystal particles of MA were prepared using an antisolvent precipitation technique. In the process, Kollidon VA 64 and Poloxamer 407 in aqueous phase were employed as a hydrophilic polymer and a surfactant, respectively, to inhibit crystal growth and aggregation, resulting in the transformation of morphology (crystal habit) of the processed MA microcrystals. Particle size was affected by the type of polymer or surfactant used and the concentration of either the polymer or drug. The dissolution properties of the processed MA microcrystal particles were enhanced in comparison with those of the unprocessed drug by increasing the surface area caused by a reduction in particle size. These results illustrate that this antisolvent precipitation technique in mild conditions allows for processed MA microcrystals with a reduced particle size, a narrow particle size distribution and enhanced dissolution properties. This technique is a promising and economical method for the preparation of submicron drug particles for commercial procedures.

Acknowledgments

This work was supported by the National Research Foundation of Korea (NRF) grant funded by the Korea government (MEST) (No. 2008-0060533), Priority Research Centers Program through the National Research Foundation of Korea (NRF) funded by the Ministry of Education, Science and Technology (2009-0093815) and, in part, by a grant of the Korea Healthcare Technology R&D Project, Ministry for Health, Welfare and Family Affairs, Republic of Korea (A080470).

References

Ali, H.S.M., York, P., Blagden, N., 2009. Preparation of hydrocortisone nanosuspension through a bottom-up nanoprecipitation technique using microfluidic reactors. Int. J. Pharm. 375, 107–113.
Bilati, U., Allémann, E., Doelker, E., 2005. Development of a nanoprecipitation method intended for the entrapment of hydrophilic drugs into nanoparticles. Eur. J. Pharm. Sci. 24, 67–75.
Blagden, N., Matas, M.de., Gavan, P.T., York, P., 2007. Crystal engineering of active pharmaceutical ingredients to improve solubility and dissolution rates. Adv. Drug Deliv. Rev. 59, 617–630.
Brittain, H.G., 1999. Polymorphism in Pharmaceutical Solids. Dekker, New York.
Chen, H., Khemtong, C., Yang, X., Chang, X., Gao, J., 2010. Nanonization strategies for poorly water-soluble drugs. Drug Discov. Today.
Chen, X., Young, T.J., Sarkari, M., Williams III, R.O., Johnston, K.P., 2002. Preparation of cyclosporine A nanoparticles by evaporative precipitation into aqueous solution. Int. J. Pharm. 242, 3–14.
Chen, X., Matteucci, M.E., Lo, C.Y., Johnston, K.P., 2009. Flocculation of polymer stabilized nanocrystal suspensions to produce redispersible powders. Drug Dev. Ind. Pharm. 35, 283–296.
Cushing, B.L., Kolesnichenko, V.L., O'Connor, C.J., 2004. Recent advances in the liquid-phase syntheses of inorganic nanoparticles. Chem. Rev. 104, 3893–3946.
Dong, Y., Ng, W.K., Shen, S., Kim, S., Tan, R.B.H., 2009. Preparation and characterization of spironolactone nanoparticles by antisolvent precipitation. Int. J. Pharm. 375, 84–88.
Dukhin, S.S., Shena, Y., Davea, R., Pfeffera, R., 2007. Development in modeling submicron particle formation in two phases flow of solvent-supercritical antisolvent emulsion. Adv. Colloid Interface Sci. 134–135, 72–88.
Goddeeris, C., Coacci, J., Van den Mooter, G., 2007. Correlation between digestion of the lipid phase of smedds and release of the anti-HIV drug UC 781 and the antimycotic drug enilconazole from smedds. Eur. J. Pharm. Biopharm. 66, 173–181.
Goddeeris, C., Willems, T., Van den Mooter, G., 2008. Formulation of fast disintegrating tablets of ternary solid dispersions consisting of TPGS 1000 and HPMC 2910 or PVPVA 64 to improve the dissolution of the anti-HIV drug UC 781. Eur. J. Pharm. Sci. 34, 293–302.
Hargrove, J.T., Maxson, W.S., Wentz, A.C., 1989. Absorption of oral progesterone is influenced by vehicle and particle size. Am. J. Obstet. Gynecol. 161, 948–951.
Hovey, D., Pruitt, T., Ryde, T., 2005. Nanoparticulate megestrol formulations. US Patent 2005/0233001 A1, 20 October.
Huang, Q.-P., Wang, J.-X., Chen, G.-Z., Shen, Z.-G., Chen, J.-F., Yun, J., 2008. Micronization of gemfibrozil by reactive precipitation process. Int. J. Pharm. 360, 58–64.
Keck, C.M., Muller, R.H., 2006. Drug nanocrystals of poorly soluble drugs produced by high pressure homogenisation. Eur. J. Pharm. Biopharm. 62, 3–16.
Kim, J.-S., Kim, M.-S., Park, H.J., Jin, S.-J., Lee, S., Hwang, S.-J., 2008a. Physicochemical properties and oral bioavailability of amorphous atorvastatin hemi-calcium using spray-drying and SAS process. Int. J. Pharm. 359, 211–219.
Kim, M.-S., Jin, S.-J., Kim, J.-S., Park, H.J., Song, H.-S., Neubert, R.H.H., Hwang, S.-J., 2008b. Preparation, characterization and in vivo evaluation of amorphous atorvastatin calcium nanoparticles using supercritical antisolvent (SAS) process. Eur. J. Pharm. Biopharm. 69, 454–465.
Kipp, J.E., 2004. The role of solid nanoparticle technology in the parenteral delivery of poorly water-soluble drugs. Int. J. Pharm. 284, 109–122.
Kocbek, P., Baumgartner, S., Kristl, J., 2006. Preparation and evaluation of nanosuspensions for enhancing the dissolution of poorly soluble drugs. Int. J. Pharm. 312, 179–186.
Kondo, M., Niwa, T., Okamoto, H., Banjo, K., 2009. Particle characterization of poorly water-soluble drugs using a spray freeze drying technique. Chem. Pharm. Bull. 57, 657–662.
Labouret, A.de, Thioune, O., Fessi, H., Devissaguet, J.P., Puisieux, F., 1995. Application of an original process for obtaining colloidal dispersions of some coating polymers. Preparation, characterization, industrial scale-up. Drug Dev. Ind. Pharm. 21, 229–241.
Leuner, C., Dressman, J., 2000. Improving drug solubility for oral delivery using solid dispersions. Eur. J. Pharm. Biopharm. 50, 47–60.

Lim, S.-J., Kim, C.-K., 2002. Formulation parameters determining the physicochemical characteristics of solid lipid nanoparticles loaded with all-trans retinoic acid. Int. J. Pharm. 243, 135–146.
Löbenberg, R., Amidon, G.L., 2000. Modern bioavailability, bioequivalence and biopharmaceutics classification system. New scientific approaches to international regulatory standards. Eur. J. Pharm. Biopharm. 50, 3–12.
Marshall, P.V., York, P., 1989. Crystallization solvent induced solid-state and particulate modifications of nitrofurantoin. Int. J. Pharm. 55, 257–263.
Mateen, F., Jatoi, A., 2006. Megestrol acetate for the palliation of anorexia in advanced, incurable cancer patients. Clin. Nutr. 25, 711–715.
Matteucci, M.E., Hotze, M.A., Johnston, K.P., Williams III, R.O., 2006. Drug nanoparticles by antisolvent precipitation: mixing energy versus surfactant stabilization. Langmuir 22, 8951–8959.
Merisko-Liversidge, E., Liversidge, G.G., Eugene, R.C., 2003. Nanosizing: a formulation approach for poorly-water-soluble compounds. Eur. J. Pharm. Sci. 18, 113–120.
Midoux, N., Hosek, P., Pailleres, L., Authelin, J.R., 1999. Micronization of pharmaceutical substances in a spiral jet mill. Powder Technol. 104, 113–120.
Mosharraf, M., Nyström, C., 1995. The effect of particle size and shape on the surface specific dissolution rate of microsized practically insoluble drugs. Int. J. Pharm. 122, 35–47.
Nokhodchi, A., Bolourtchian, N., Dinarvand, R., 2003. Crystal modification of phenytoin using different solvents and crystallization conditions. Int. J. Pharm. 250, 85–97.
Noyes, A.A., Whitney, W.R., 1897. The rate of solution of solid substances in their own solutions. J. Am. Chem. Soc. 19, 930–934.
Park, H.J., Kim, M.-S., Lee, S.B., Kim, J.-S., Woo, J.-S., Park, J.-S., Hwang, S.-J., 2007. Recrystallization of fluconazole using the supercritical antisolvent (SAS) process. Int. J. Pharm. 328, 152–160.
Park, K.-M., Lee, M.-K., Hwang, K.-J., Kim, C.-K., 1999. Phospholipid-based microemulsions of flurbiprofen by the spontaneous emulsification process. Int. J. Pharm. 183, 145–154.
Perrut, M., Jung, J., Leboeuf, F., 2005. Enhancement of dissolution rate of poorly-soluble active ingredients by supercritical fluid processes. Part I. Micronization of neat particles. Int. J. Pharm. 288, 3–10.
Perrut, M., Clavier, J.-Y., 2003. Supercritical fluid formulation: process choice and scale-up. Ind. Eng. Chem. Res. 42, 6375–6383.
Raghavan, S.L., Kiepfer, B., Davis, A.F., Kazarian, S.G., Hadgraft, J., 2001. Membrane transport of hydrocortisone acetate from supersaturated solutions; the role of polymers. Int. J. Pharm. 221, 95–105.
Rasenack, N., Hartenhauer, H., Müller, B.W., 2003. Microcrystals for dissolution rate enhancement of poorly water-soluble drugs. Int. J. Pharm. 254, 137–145.
Rasenack, N., Muller, B.W., 2004. Micron-size drug particles: common and novel micronization techniques. Pharm. Dev. Technol. 9, 1–13.
Ruch, F., Matijevic, E., 2000. Preparation of micrometer size budesonide particles by precipitation. J. Colloid Interface Sci. 229, 207–211.
Russel, W.B., Saville, D.A., Schowalter, W.R., 1989. Colloidal Dispersions. Cambridge, New York, pp. 310–328.
Sarkari, M., Brown, J., Chen, X., Swinnea, S., Williams, R.O., Johnston, K.P., 2002. Enhanced drug dissolution using evaporative precipitation into aqueous solution. Int. J. Pharm. 243, 17–31.
Shekunov, B.Y., Chattopadhyay, P., Seitzinger, J., Huff, R., 2006. Nanoparticles of poorly water-soluble drugs prepared by supercritical fluid extraction of emulsions. Pharm. Res. 23, 196–204.
Stainmesse, S., Orecchioni, A.-M., Nakache, E., Puisieux, F., Fessi, H., 1995. Formation and stabilization of a biodegradable polymeric colloidal suspension of nanoparticles. Colloid Polym. Sci. 273, 505–511.
Thioune, O., Fessi, H., Devissaguet, J.P., Puisieux, F., 1997. Preparation of pseudolatex by nanoprecipitation: influence of the solvent nature on intrinsic viscosity and interaction constant. Int. J. Pharm. 146, 233–238.
Vivek, K., Meenakshi, B., Harish, D., Deepak, K., 2006. Nanoparticle technology for the delivery of poorly water-soluble drugs. Pharm. Dev. Technol. 30 (2), 82–92.
Wang, J., Chen, J.F., Le, Y., Shen, Z.G., 2007. Preparation of ultrafine beclomethasone dipropionate drug powder by antisolvent precipitation. Ind. Eng. Chem. Res. 46, 4839–4845.
Watari, N., Funaki, T., Aizawa, K., Kaneniwa, N., 1983. Nonlinear assessment of nitrofurantoin bioavailability in rabbits. J. Pharmacokinet. Pharmacodyn. 11, 529–545.
Won, D.-H., Kim, M.-S., Lee, S.B., Park, J.-S., Hwang, S.-J., 2005. Improved physicochemical characteristics of felodipine solid dispersion particles by supercritical anti-solvent precipitation process. Int. J. Pharm. 301, 199–208.
Yeo, S.-D., Kim, M.-S., Lee, J.-C., 2003. Recrystallization of sulfathiazole and chlorpropamide using the supercritical fluid antisolvent process. J. Supercrit. Fluids 25, 143–154.
Zhang, J.-Y., Shen, Z.-G., Zhong, J., Hu, T.-T., Chen, J.-F., Ma, Z.-Q., Yun, J., 2006. Preparation of amorphous cefuroxime axetil nanoparticles by controlled nanoprecipitation method without surfactants. Int. J. Pharm. 323, 153–160.
Zimmermann, A., Millqvist-Fureby, A., Elema, M.R., Hansen, T., Müllertz, A., Hovgaard, L., 2009. Adsorption of pharmaceutical excipients onto microcrystals of siramesine hydrochloride: effects on physicochemical properties. Eur. J. Pharm. Biopharm. 71, 109–116.